PHYSICAL REVIEW C VOLUME 25, NUMBER 1 JANUARY 1982

Self-consistent description of heavy nuclei. I. Static properties of some even nuclei

J. Libert
Centre de Spectrométrie Nucléaire et de Spectrométrie de Masse, Bâtiment 104, Campus Orsay, 91406-Orsay, France

P. Quentin
Institut Laue-Langevin, 156X, 38042 Grenoble-Cedex, France
(Received 30 June 1981)

Hartree-Fock+BCS calculations of 15 even nuclei within and around the actinide region have been performed with the Skyrme *S*III effective force. A careful optimization of the two parameters of the truncated expansion basis has been made for each nucleus. The iterative process has been carried out as far as to yield an excellent numerical convergence of quadrupole Q_2 and hexadecapole Q_4 moments (better than 0.1% for Q_2 and 1% for Q_4). Total binding energies have been reproduced up to ~ 2 MeV. Charge radii have been found in agreement with experimental data to $\sim 1\%$, whereas the error on Q_2 and Q_4 moments (for $A \leq 240$) were less than 5% and 25%, respectively. Single particle Hartree-Fock energy spectra are discussed and will be compared with experimental data in a subsequent paper. Finally, the deformation energy curves of two nuclei (^{232}Th and ^{240}Pu) are displayed.

[NUCLEAR STRUCTURE 15 heavy even nuclei from ^{224}Ra to ^{260}104 studied within Hartree-Fock+BCS using Skyrme *S*III force. Binding energies, charge radii, quadrupole and hexadecapole moments, single particle energies calculated. Numerical convergence assessed.]

I. INTRODUCTION

Hartree-Fock+Bardeen-Cooper-Schrieffer (BCS) calculations using phenomenological effective interactions of the Skyrme type have been very successful in describing many nuclear static properties for spherical,[1,2] transitional,[3–8] and well deformed nuclei.[9–12] In this paper we will extend such calculations to very heavy deformed nuclei, i.e., for nuclei within and around the actinide region.

As pointed out in Ref. 2 there exists an infinity of Skyrme forces (defined by five parameters for the central part of the force) yielding correct nuclear matter saturation properties. However, the amount of velocity dependence characterizes completely such a force. The Skyrme *S*III force which we will use here, corresponds to an effective mass in nuclear matter which is equal to about $\frac{3}{4}$ of the nucleonic mass. Such a value seems consistent, particularly with the properties of the giant isoscalar quadrupole resonances,[13] and is needed for a phenomenological reproduction of the single particle level density in deformed nuclei.[12] The latter property will be used in a subsequent paper,[14] hereafter referred to as II, where a systematic estimation of the spectroscopic properties of odd actinide nuclei will be achieved by coupling the quasiparticle states determined in this work with a rotational core fitted to even-even neighboring nuclei.

In view of the wealth of publications dealing with Hartree-Fock+BCS calculations using Skyrme effective forces (for a comprehensive discussion of their results see, e.g., Ref. 15), it is not necessary to present here any technical details about the method in use. We will instead insist now on some specific features of the present calculations. We have performed Hartree-Fock+BCS calculations of ground state properties for 15 nuclei ranging from $Z = 88 - 104$ (see Fig. 1). The Hartree-Fock single-particle states have been expanded on an axially symmetrical harmonic oscillator basis including about 13 major oscillator

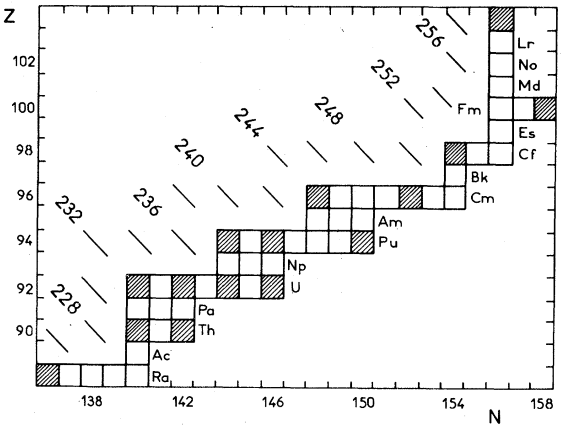

FIG. 1. Heavy nuclei whose ground state properties have been calculated in this work (figured in hatched boxes).

shells. For each nucleus we have determined (see Appendix A) the basis parameters b and q (with the notation of Ref. 3) yielding the lowest total energy. These optimal parameters are listed in Table I. The sensitivity of various observables with respect to these parameters is discussed in Appendix A, from explicit calculations of a specific example. The nonlinear variational equations are solved iteratively. Starting from a standard Woods-Saxon ansatz for the Hartree-Fock mean field, it has been found necessary, as discussed in Appendix A, to perform 50 interations to extrapolate safely the converged values of quadrupole Q_2 and hexedecapole Q_4 moments with an accuracy $\lesssim 0.1\%$ for Q_2 and $\lesssim 1\%$ for Q_4. Pairing correlations have been included through a simplified BCS approximation[9] consisting in the imposition of definite values to the neutron and proton pairing gaps. These values, determined from the systematics of odd-even binding energy differences,[16] are listed in Table I. As was done for the basis parameters, the influence of a small variation of these gaps around the values in use is discussed in Appendix A. For the nucleus ^{232}Th we have performed constrained Hartree-Fock calculations according to the method discussed in Ref. 3. In this case, optimal basis parameters have been exactly determined for three points in the deformation energy curve (for the spherical point and at the prolate and oblate local minima); otherwise they have been deduced from a linear (in Q_2) interpolation or extrapolation. Along this curve, pairing correlations have been taken into account within the approximation of a constant pairing matrix element G assumed to be deformation independent (for a critical discussion of this approximation see, e.g., Ref. 5).

In Sec. II, calculated total binding energies will be compared with experimental ones. The deformation energy curve of ^{232}Th will be presented. Finally, the calculated single-particle energy spectra will be discussed. Section III will be devoted to a survey of calculated nuclear densities. Radii and quadrupole and hexadecapole moments will be compared with available experimental data and the

TABLE I. Basis parameters (b and q with the notation of Ref. 3) and neutron and proton pairing gaps (Δ_n and $\Delta_p I$). The parameter q is dimensionless, b is expressed in fm^{-1}, and the gaps are given in MeV.

Nucleus	b	q	Δ_n	Δ_p
^{224}Ra	0.507	1.15	0.76	0.95
^{230}Th	0.498	1.13	0.77	0.97
^{232}Th	0.494	1.22	0.75	0.95
^{232}U	0.487	1.22	0.69	0.87
^{234}U	0.486	1.24	0.68	0.86
^{236}U	0.485	1.28	0.64	0.91
^{238}U	0.485	1.28	0.60	0.85
^{238}Pu	0.514	1.23	0.60	0.74
^{240}Pu	0.489	1.25	0.57	0.76
^{244}Pu	0.489	1.25	0.30	0.78
^{244}Cm	0.483	1.27	0.59	0.98
^{248}Cm	0.483	1.27	0.02	1.04
^{252}Cf	0.488	1.20	0.62	0.87
^{258}Fm	0.477	1.35	0.62	0.87
^{260}104	0.513	1.275	0.60	0.85

results of previous theoretical estimates. As already noted we will discuss in Appendix A the accuracy and the convergence of our calculations, whereas Appendix B will shortly specify the way in which standard β_2, β_4 deformation parameters have been extracted out of our wave functions.

II. ENERGIES

Total binding energies as resulting from our calculations must first be corrected for truncation effects. The corresponding lack of binding energy may be evaluated for the size of the basis in use (13 shells) and for some spherically symmetric solutions where exact solutions[1] of the Hartree-Fock equations are available. One finds 7.75 MeV for ^{208}Pb and 8.50 MeV for ^{240}Pu. Upon assuming this truncation effect to vary linearly with A and to be deformation independent, one can approximately correct our calculated Hartree-Fock energies. These energies, however, are merely intrinsic energies and thus contain a spurious rotational energy which in the pure rotational limit is found equal to

$$E_{\text{intrinsic}} - E_{0^+} = \frac{\hbar^2}{2I} \langle \psi_{\text{intrinsic}} | \vec{J}^2 | \psi_{\text{intrinsic}} \rangle \ . \qquad (1)$$

Both the expectation value of the square of the angular momentum $\vec{J}^2$ and the moment of inertia I have been calculated recently[17] for 6 Hartree-Fock solutions and within the Inglis Cranking formalism (for I). Whereas the rotational hypothesis is fully justified for nuclei such as ^{236}U and for "transitional" nuclei such as ^{224}Ra or even ^{230}Th, Eq. (1) is only meant to provide us with a rough estimate. In Table II, we compare uncorrected, corrected for truncation, corrected for 0^+ projection, and experimental[18] energies. Without correcting for the spurious rotational energy one notices a systematical lack of binding of $\sim$4 MeV. Roughly half of it can be accounted for by the correction of Eq. (1). As a conclusion, whereas for magic nuclei[2] the calculated and experimental binding energies agree within $\sim \pm 0.5$ MeV, for well deformed nuclei the Skyrme SIII force leads consistently to an underestimation of $\sim$2 MeV.

In Fig. 2 we have plotted the deformation energy curve of the ^{232}Th nucleus. In the same figure we have also given the deformation energy curve of ^{240}Pu (taken from Ref. 19 for the prolate part and Ref. 20 for the oblate part). For the sake of comparison between these two curves, we have chosen $Q_2 A^{-5/3}$ (where A is the nucleon number) as the deformation parameter. The ^{232}Th curve exhibiting a prolate-oblate energy difference of $\sim$4.5 MeV and a spherical barrier (versus the prolate minimum) of $\sim$6 MeV is a typical example of deformation energy curves at the beginning of a nuclear rigid deformation region. The ^{240}Pu nucleus in turn appears as a good example of a rigid rotor

TABLE II. Calculated binding energies (in MeV). Calculated binding energies resulting from our calculations, corrected for truncation effects and corrected also for 0^+ projection effects are compared with available experimental data (Ref. 18). In the ^{260}104 case the energy listed as an experimental one is deduced from systematics.

Binding energies	Calculated ($N=12$)	Corrected for truncation	Corrected for 0^+ projection	Experimental
^{224}Ra	−1708.1	−1716.2	−1717.8	−1720.3
^{230}Th	−1743.8	−1752.1	−1754.0	−1755.2
^{232}Th	−1754.8	−1763.1		−1766.7
^{232}U	−1753.2	−1761.5		−1766.0
^{234}U	−1766.0	−1774.4		−1778.6
^{236}U	−1777.8	−1786.2	−1788.1	−1790.4
^{238}U	−1788.9	−1797.4		−1801.7
^{238}Pu	−1790.3	−1798.8		−1801.3
^{240}Pu	−1800.5	−1809.0		−1813.5
^{244}Pu	−1823.2	−1831.8		−1836.1
^{244}Cm	−1823.9	−1832.5	−1834.4	−1835.9
^{248}Cm	−1847.7	−1856.4	−1858.4	−1859.2
^{252}Cf	−1868.4	−1877.2		−1881.3
^{258}Fm	−1900.3	−1902.2	−1911.5	
^{260}104	−1906.7	−1915.7		−1918.0

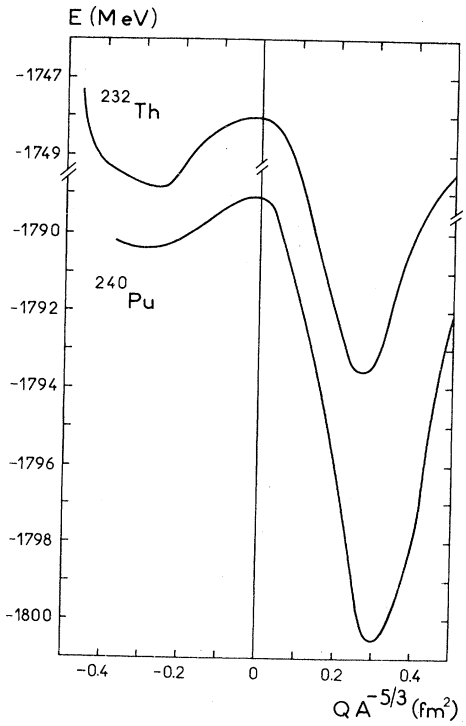

FIG. 2. Deformation energy curves for the ^{232}Th and ^{240}Pu isotopes. The deformation parameter is the mass quadrupole moment Q divided by $A^{5/3}$, where A is the nucleon number. This parameter has been chosen in such a way as to allow a direct comparison of deformation properties for nuclei with different A values.

(high prolate-oblate energy difference and high spherical barrier), which provides an *a priori* justification of the core plus quasiparticle coupling calculations performed in II. Consistent with the previous remarks one notices that values of $Q_2A^{-5/3}$ for both the prolate and the oblate minima are smaller for the ^{232}Th nucleus than for the ^{240}Pu nucleus.

The evolution of the neutron and proton single particle spectra as a function of the deformation is shown in Figs. 3 and 4, respectively. The spherical neutron level sequence obtained with the Skyrme *S*III force may be discussed in terms of those obtained in more phenomenological approaches consisting in the assumption of a central Hartree-Fock mean field as being a Woods-Saxon potential,[21] a folded Yukawa potential,[22] or a modified harmonic oscillator.[23,24] In what follows we compare our Fig. 3 with Fig. 11 of Ref. 21, Fig. 1(b) of Ref. 22, and Fig. 4 of Ref. 24. The first two wells have been determined for the ^{240}Pu nucleus. Their resulting spectra compare well with ours; they indeed yield similar spacings (1.5 MeV) between the $1i\,\frac{11}{2}$ and $1j\,\frac{15}{2}$ states. However, they produce $2g\,\frac{9}{2}$ states very close to the $1i\,\frac{11}{2}$ states, contrary to our calculations (where the $2g\,\frac{9}{2}$ state lies just in the middle of the $1i\,\frac{11}{2}$ and $1j\,\frac{15}{2}$ states). The results of Ref. 24 are in slight disagreement with ours since they predict almost degenerate $1i\,\frac{11}{2}$ and $1j\,\frac{15}{2}$ states and a $2g\,\frac{9}{2}$ state lying about 1.5 MeV lower (assuming the harmonic osillator frequency to be given by $\hbar\omega \sim 41\,A^{-1/3}$ MeV (Ref. 30). In the calculations of Ref. 24 the hexadecapole (and more generally multipole other than quadrupole) deformation parameter ϵ_4 is set equal to zero. The inclusion of a more realistic value ($\epsilon_4 \sim -0.04$) is not expected to dramatically change the level ordering as can be seen from Fig. 2(f) of Ref. 23.

The proton spectrum of Fig. 4 agrees very well with the one given in Fig. 10 of Ref. 21. A qualitative agreement is also obtained when comparing our Fig. 4 with Fig. 1(a) of Ref. 22 and Fig. 3 of Ref. 24. Indeed, the energy difference between the $1h\frac{9}{2}$ and the ($2f\,\frac{7}{2}$, $1i\,\frac{13}{2}$) states is found to be ~ 1 MeV in both phenomenological approaches instead of ~ 3 MeV in our case, and similarly for the spacing between the ($3s\,\frac{1}{2}$, $2d\,\frac{3}{2}$) and ($2f\frac{7}{2}$, $1i\,\frac{13}{2}$) states where we obtain 6 MeV instead of $\sim$ 4 MeV in Refs. 22 and 24.

As already observed[3] the deformation dependence of the Hartree-Fock single-particle energies is very similar to what is obtained in more phenomenological approaches as in the Nilsson modified oscillator model. Therefore, the spherical level ordering is the most important *a priori* feature for discriminating between different mean fields. A better and *a posteriori* criterium consists indeed in comparing the deformed single-particle spectrum with available spectroscopic data on odd nuclei once the pairing and rotation-particle coupling effects have been properly taken into account. For the results of such a comparison we refer to II.

The results presented in Figs. 3 and 4 correspond to the ^{232}Th nucleus. When changing slightly the number of neutrons and protons at a given deformation, one generally observes only small changes in the relative ordering of levels. However, if one is interested in the ground state single particle sequence, one has to take into account the variation of the mean field deformation when going from one nucleus to another. This is exemplified in Figs. 5 and 6 for the ground state neutron and proton spectra, respectively, of seven nuclei (^{224}Ra,

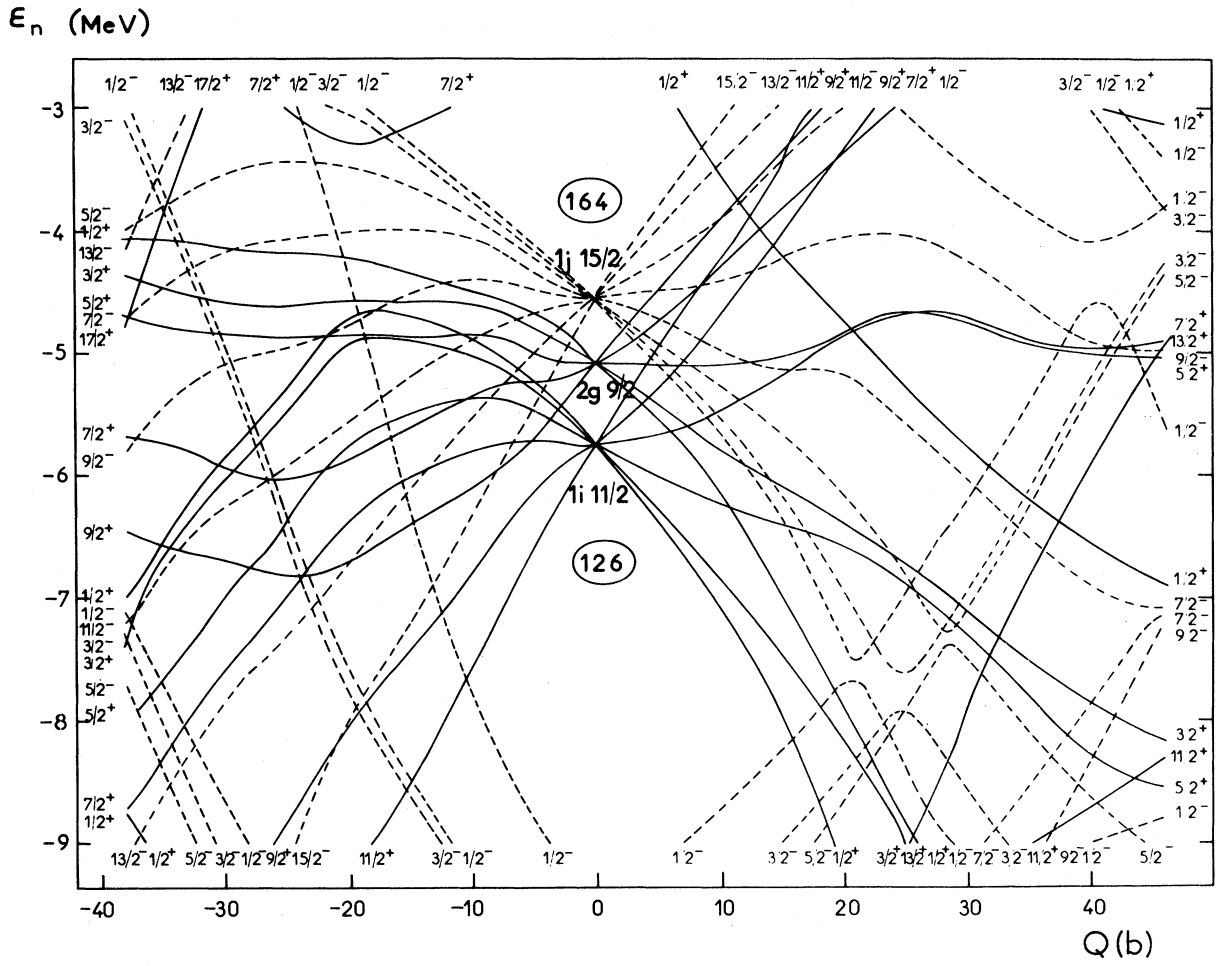

FIG. 3. Neutron single particle energies as functions of the mass quadrupole moment Q (in barn) calculated for the ^{232}Th nucleus. Each level is labeled by its Ω^{π} value where Ω is the projection of its total (orbital+spin) angular momentum and π its parity.

^{232}Th, ^{236}U, ^{240}Pu, ^{244}Cm, ^{252}Cf, and ^{260}104).

The recent spectroscopic data on odd fission isomers undoubtedly constitute a challenging testing ground for any theoretical estimate of deformed mean fields. At such exotic deformations ($\beta_2 \sim 0.6$) one is testing nuclear properties very far from those which have been used to make a phenomenological adjustment of the six effective force parameters. However, it turns out[25] that using the quasiparticle states deduced from our self-consistent solutions. In Fig. 7, we compare the Hartree-Fock single particle spectrum obtained with the Skyrme *SIII* force for the ^{240}Pu fission isomer, and those stemming from three phenomenological approaches.[26] For the spectroscopic properties under study in Ref. 25, the correct location of the $\frac{9}{2}^-$ and the neighboring $\frac{5}{2}^+$ single particle states has been found essential. In this respect, one sees in Fig. 7 that the phenomenological approach of Ref. 22 compares very favorably with our results, and thence, with experimenal data.

III. DENSITIES

In this section, we will present our calculated nuclear densities through some of their moments (radii and quadrupole and hexadecapole moments). The actual charge distribution *a priori* differs from the point proton distribution by the proton form factor. Upon assuming the latter to be of a mono-

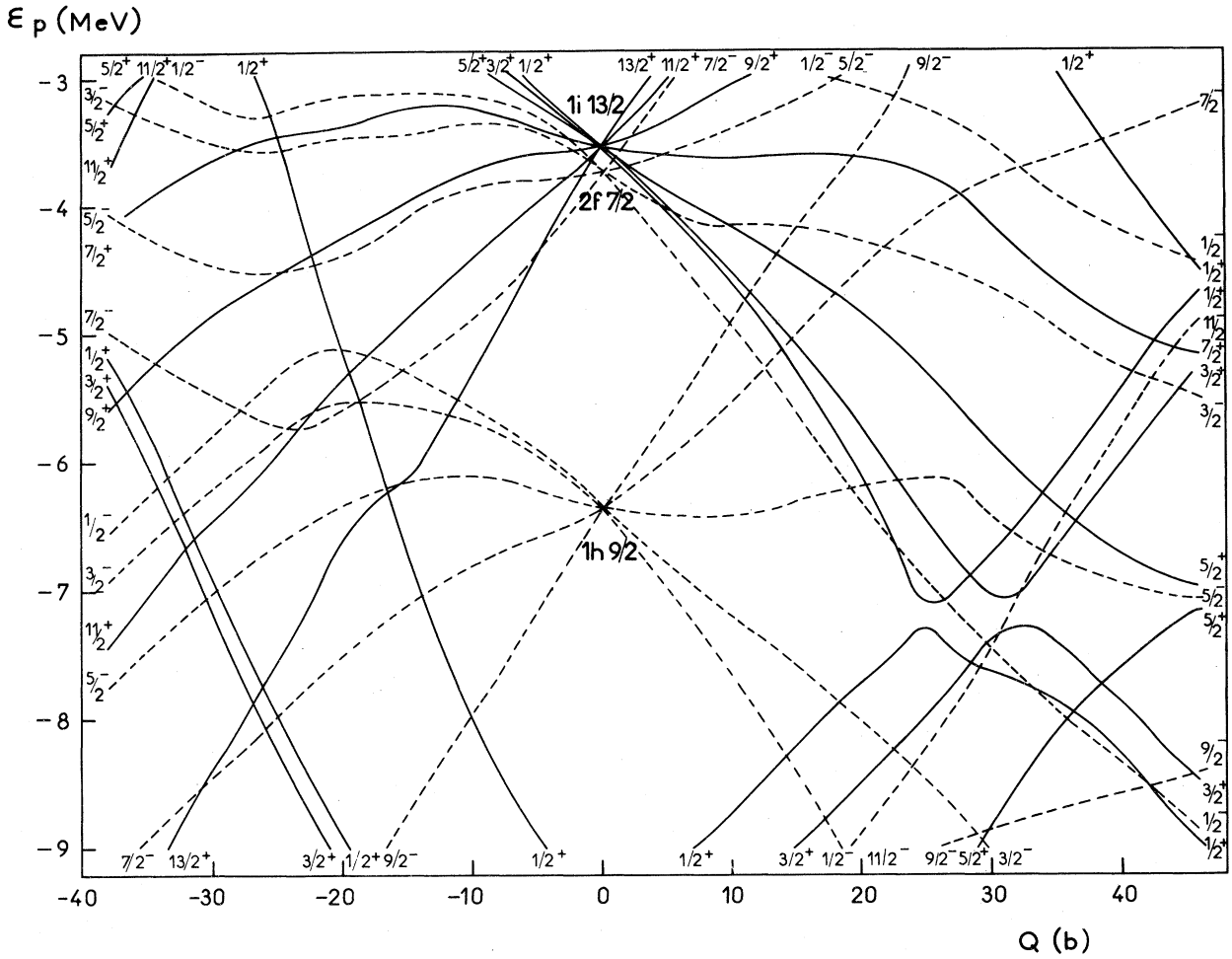

FIG. 4. Same as Fig. 3 for protons.

polar character, it can be shown[27,28]—as we will shortly recall in Appendix B—that the two distributions, however, have the same multipole moments, but different radii. The latter are given by

$$r_{\text{charge}}{}^2 = r_{\text{point charge}}{}^2 + r_{\text{proton}}{}^2 , \tag{2}$$

where $r_{\text{proton}}{}^2 \simeq 0.64$ fm^2 and $r_{\text{point charge}}{}^2$ is obtained from the calculated proton density $\rho(\vec{r})$ by

$$r_{\text{point charge}}{}^2 = \frac{1}{A} \int d^3\vec{r}\, \rho(\vec{r}) r^2 . \tag{3}$$

For such heavy nuclei the bad treatment of the center of mass motion affects only slightly the results of the integral in Eq. (3). Indeed, upon assuming pure harmonic oscillator wave functions one gets[27] a corrective term for the charge radius ($r \equiv r_{\text{point charge}}$) given by

$$\frac{\delta r}{r} = \frac{2(\hbar^2/2m)}{r_0{}^2 \hbar\omega A^{5/3}} q^{-1/3} \left[\frac{2+q}{3} \right] , \tag{4}$$

where q is the deformation parameter, ω is the harmonic oscillator frequency, and r_0 is the radius liquid drop constant. For ^{240}Pu, where $q = 1.25$ (see Table I) and with $r_0 = 1.2049$ fm (Ref. 29) and $\hbar\omega = 41 A^{-1/3}$ MeV (Ref. 30), one gets

$$\frac{\delta r}{r} \simeq 0.0005 , \tag{5}$$

yielding an overestimation of the radius by $\simeq 0.003$ fm.

Charge radii values corrected as specified in Eq. (5) have been listed in Table III (no corrections for the neutron charge form factor or for relativistic Coulomb effects[31] have been taken into account). As compared with experimental available data[32] our results are found too large by 1.2—1.4 % as was previously observed in medium and heavy spherical and deformed nuclei (see Table V of Ref. 15).

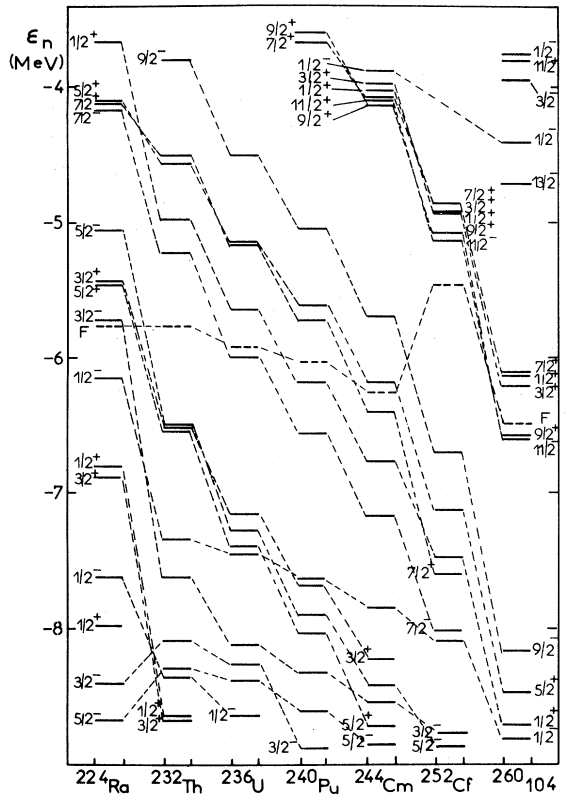

FIG. 5. Neutron single particle energies for various nuclei calculated at their ground state. Each level is labeled by its Ω^{π} value as in Figs. 3 and 4. The Fermi level F is represented by a dashed line.

In Table III we have reported quadrupole and hexadecapole moments of the calculated charge densities. They correspond to the following operators (with usual notation):

$$Q_2 = \langle 2r^2 P_2(\cos\theta) \rangle \ , \qquad (6)$$

$$Q_4 = \langle r^4 Y_{40}(\theta) \rangle \ .$$

They are compared with intrinsic Q_2 values deduced from a systematic evaluation of $B(E2)$ data[33] and with intrinsic Q_4 values deduced from $\langle ||\mathcal{M}(E4)|| \rangle$ Coulomb excitation measurements.[34] Our calculated Q_2 values are slightly underestimating the data but reproduce very well their overall trend. The agreement with Q_4 experimental values is also very good up to $A \sim 240$. For the heavier elements so far experimentally studied, our calculations are unable to reproduce the dramatic decrease of Q_4 to about a zero value.

In order to make contact with the experimental means of determining deformation properties (such

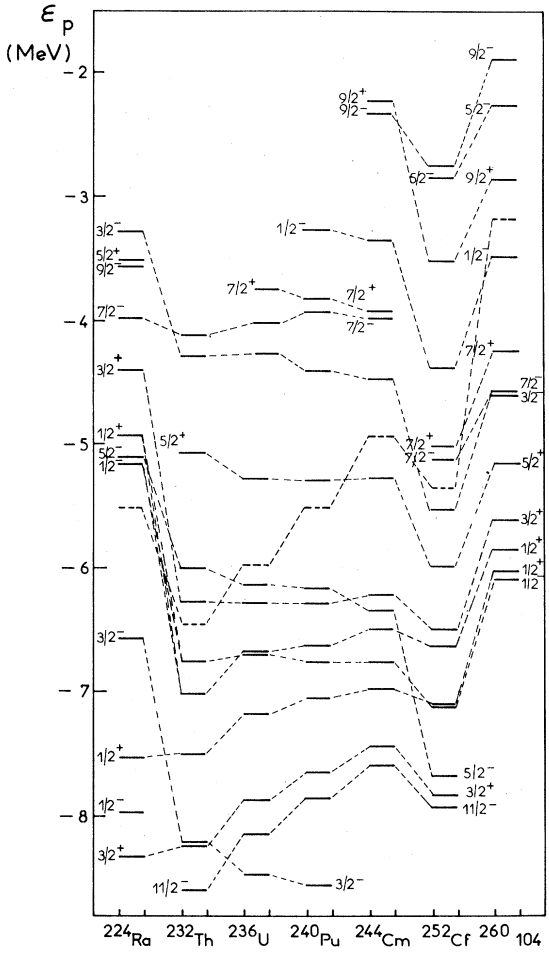

FIG. 6. Same as Fig. 5 for protons.

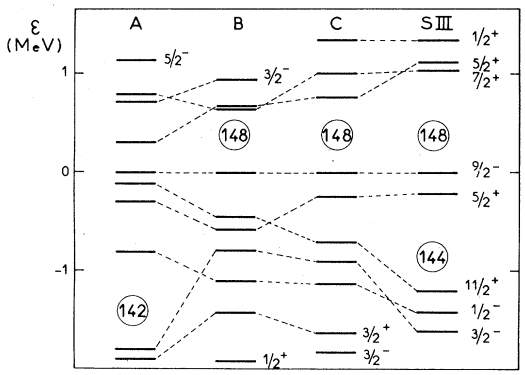

FIG. 7. Neutron single particle energies calculated for the ^{240}Pu nucleus at the fission isomeric state. Each level is labeled by its Ω^{π} value as in Figs. 3 and 4. Our results are labeled by *SIII*. Other results come from the following phenomenological approaches: Ref. 21 for *A*, Mosel and Schmitt, Nucl. Phys. A165 13 (1971) for *B*, and Ref. 22 for C.

TABLE III. Comparison of calculated and experimental moments of the charge distribution. Radii r are expressed in fm, quadrupole moments Q_2 in b, hexadecapole moments, Q_4 in b^2. For the experimental data see Refs. 32–34 for r, Q_2, and Q_4, respectively.

Nucleus	r^{calc}	r^{exp}	Q_2^{calc}	Q_2^{exp}	Q_4^{calc}	Q_4^{exp}
^{224}Ra	5.766		5.78	6.25±0.22	0.69	
^{230}Th	5.850		8.57	9.00±0.06	1.11	1.09±0.15
^{232}Th	5.867	5.787	9.10	9.62±0.05	1.09	1.22±0.15
^{232}U	5.884		9.71	9.95±0.60	1.20	
^{234}U	5.895		9.88	10.47±0.05	1.10	1.40±0.20
^{236}U	5.907		10.07	10.80±0.07	0.99	1.30±0.22
^{238}U	5.920	5.847	10.30	11.12±0.07	0.92	0.83±0.22
^{238}Pu	5.944		11.14	11.27±0.08	1.22	1.38±0.25
^{240}Pu	5.952		11.13	11.58±0.08	1.08	1.15±0.28
^{244}Pu	5.973		11.22	11.70±0.08	0.87	$0.03\pm^{+0.50}_{-0.80}$
^{244}Cm	5.991		11.82	12.11±0.08	0.92	$0.0\ \pm^{+0.3}_{-0.5}$
^{248}Cm	6.009		12.00	12.28±0.08	0.71	$0.0\ \pm^{+0.5}_{-0.6}$
^{252}Cf	6.045		12.04		0.57	
^{258}Fm	6.091		12.06		0.25	
^{260}104	6.128		12.84		0.21	

as hadron or electron scattering and muonic atom x-ray spectroscopy) one is forced to extract out of computed Q_2, Q_4 values standard deformation parameters β_2, β_4 á la Bohr-Mottelson. In order to do that, one has to introduce as an intermediate step a sharp-edged liquid drop defined by a radius parameter r_0 [which we will take, as before, equal to 1.2049 fm (Ref. 29)] and the two deformation parameters β_2 and β_4. The latter, which are the unknown quantities, will be fixed by demanding that the drop should have the same Q_2, Q_4 moments as our self-consistent solutions (see Appendix B for details). The non–sharp-edge character of this solution does not influence the results if one assumes the nuclear surface diffuseness to be produced by convoluting a step function with a monopole form factor—see again the discussion of Appendix B. Now, one could *a priori* ask whether it makes sense at all to compare data coming from hadronic scattering and electron scattering or Coulomb excitation experiments since one is probing in one case the matter density and in the other case only the charge density. As a result of the present work as well as of all previous similar theoretical estimations of the same kind, no significant difference between the two densities has ever been found.

Our results for the β_2 and β_4 deformation parameters of the mass distributions have been plotted in Figs. 8 and 9, respectively. The trend of the quadrupole deformation parameter is typical of the opening of a permanent deformation region up to plutonium isotopes. From curium to $Z=104$ isotopes, the calculated plateau is characteristic of a mid-shell situation. The hexadecapole deformation parameter varies with A as expected from what is known in the rare-earth region.[10] The β_4 value reaches a maximum near thorium isotopes (which is very similar to what is found for samarium isotopes) and then regularly decreases to cross the $\beta_4=0$ axis near californium isotopes (which play thus for actinide nuclei the role of erbium or yterbium isotopes).

As done in Table IV, when comparing calculated β_4 values with experimental values[34–42] one is struck by the apparent inconsistency of the latter. Even limiting oneself to hadronic scattering only,

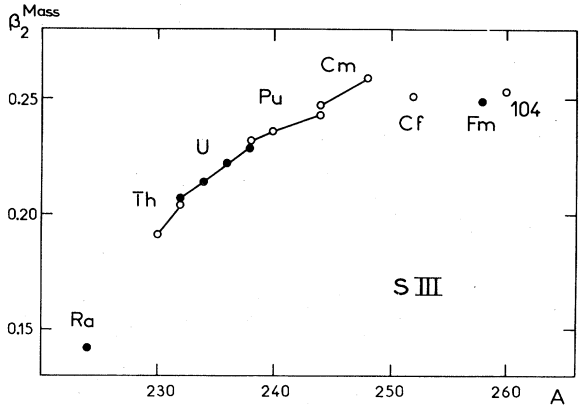

FIG. 8. Calculated ground state quadrupole deformation parameter of the mass distribution.

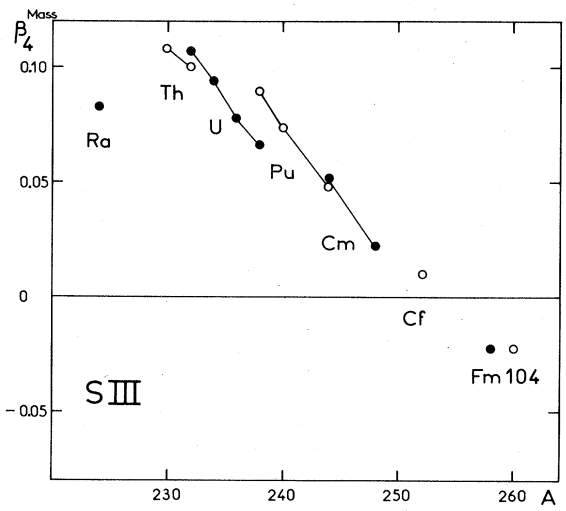

FIG. 9. Calculated ground state hexadecapole deformation parameter of the mass distribution.

one observes that upon varying the nature or the energy of the projectile one produces completely different results. A possible explanation, supported by a detailed analysis or our self-consistent wave function in the ^{238}U case,[43] might lie in the fact that the β_4 deformation parameter varies considerably in the nuclear surface. Since the penetrability of the hadronic probe depends on its nature as well as on its energy it has been possible to qualitatively correlate higher β_4 values data in ^{238}U to more peripheral scattering experiments.

In Table V we compare our calculated Q_2 and Q_4 moments for the four uranium isotopes under study here, with similar results obtained in other self-consistent calculations[44,45] or in more phenomenological approaches[22,46,47] using the Strutinsky method to determine the equilibrium points of deformation energy surfaces. Since only β_2 and β_4 values have been given in Refs. 22 and 47, we have deduced Q_2 and Q_4 values in these cases through the already discussed sharp-edged density model (with $r_0=1.2049$ fm). All theoretical estimations of Q_2 values are in good agreement between them (and with experimental data). Calculated Q_4 values are also similar, with the exception of the consistently too high values of Ref. 46. It should be noted that all the other theoretical approaches[22,46,47] have been as unsuccessful as ours in reproducing the low Q_4 values of Ref. 34 for nuclei with $A \geq 244$. In the ^{238}U case the two self-consistent calculations of Refs. 44 and 45 performed with effective forces which are very different from ours yield, however, strikingly similar Q_2 and Q_4 moments.

IV. CONCLUSIONS

The phenomenological effective Skyrme *SIII* force has been essentially fitted on the saturation properties of some magic nuclei. However, it has been shown that this force was able to reproduce the static properties of the deformed nuclei of the rare earth region. The aim of the present work was mainly to see if such a reproduction would be also obtained in the next region of rigid deformation, i.e., in the actinide region.

Before attempting an answer to such a question, one should first carefully study technical problems related to the numerical solution of the Hartree-Fock variational equations. This is why special care has been devoted to optimize the parameters of the truncated expansion basis as well as to guarantee a good convergence of the iterative numerical process. The latter is particularly impor-

TABLE IV. Comparison of calculated β_4 deformation parameters with those deduced from various hadronic scattering (α-α', p-p', n-n') experiments, muonic atom x-ray measurements, inelastic electron scattering data, and Coulomb excitation experiments. Experimental references should read as follows: (a): Ref. 36, (b): Ref. 35, (c): Ref. 37, (d): Ref. 38, (e): Ref. 42, (f): Ref. 40, (g): Ref. 41, (h): Ref. 39, (i): Ref. 34. The n-n' results published in Ref. 42 were obtained by setting $\beta_6=0$. With $\beta_6=-0.005$ these authors got recently (private communication) a similar agreement with the experimental data for the same β_2 value but with β_4 reduced to the values quoted in the Table under the label e'.

Nucleus	Theoretical	α-α'	p-p'	n-n'	μ-atoms	e-e'	Coul. exc.
^{232}Th	0.100	0.049 ± 0.010^{a}	0.050 ± 0.015^{c}	0.071 ± 0.003^{e}	0.035^{f}	0.101 ± 0.003^{h}	0.118 ± 0.018^{i}
				$0.06^{e'}$	0.001 ± 0.012^{g}		
^{234}U	0.094	0.047 ± 0.010^{a}					0.129 ± 0.023^{i}
^{236}U	0.078	0.043 ± 0.010^{a}					0.113 ± 0.026^{i}
^{238}U	0.066	0.028 ± 0.003^{a}	0.044 ± 0.004^{d}	0.057 ± 0.003^{e}	0.013^{f}	0.087 ± 0.003^{h}	0.055 ± 0.027^{i}
		$0.06\ \pm0.1^{b}$	$0.017^{+0.015}_{-0.030}{}^{c}$	$0.04^{e'}$	0.001 ± 0.012^{g}		

TABLE V. Comparison of calculated quadrupole Q_2 and hexadecapole Q_4 moments expressed in b and b^2, respectively. Our results are compared with those obtained in various other approaches: (a): Ref. 46, (b): Ref. 47, (c): Ref. 22, (d): Ref. 44 (e): Ref. 45. For the case of Refs. 22 and 47, the moments have been deduced from published β_2 and β_4 parameter values assuming a liquid drop radius constant $r_0=1.2049$ fm (Ref. 29).

Nucleus	Q_2 Present work	Q_2 Other calc.	Q_4 Present work	Q_4 Other calc.
		8.5[a]		1.2[a]
^{232}U	9.71	8.9[b]	1.20	1.0[b]
		9.5[c]		1.3[c]
		9.1[a]		1.2[a]
^{234}U	9.88	9.4[b]	1.10	1.0[b]
		9.8[c]		1.2[c]
		9.8[a]		1.3[a]
^{236}U	10.07	10.1[b]	0.99	1.0[b]
		10.0[c]		1.1[c]
		10.4[a]		1.4[a]
^{238}U	10.30	10.2[b]	0.92	0.9[b]
		10.0[c]		1.0[c]
		10.4[d]		1.0[d]
		10.4[e]		0.9[e]

tant for the precise determination of multipole moments. We have carried through the iterations in such a way as to determine results with an accuracy of $\sim 0.1\%$ for Q_2 moments and $\sim 1\%$ for Q_4 moments.

Calculated binding energies (typically equal to 1800) have been reproduced up to ~ 2 MeV. The deformation energy curves of two nuclei (^{232}Th and ^{240}Pu) have been compared and found to be typical of a beginning of a shell and of a mid-shell deformed nucleus. Single-particle Hartree-Fock energy spectra have been displayed and will be discussed in II.

The agreement of charge radii with experimental data has been found to be excellent; the relative error has been shown not to exceed 1.4%. The trend of the variation with respect to the numbers of neutrons and protons of the Q_2 and Q_4 moments has been very well reproduced. The absolute (rms) errors are 0.52 b for Q_2 and 0.19 b^2 for Q_4. In the latter case we have only taken into account isotopes with $A \leq 240$. Indeed, for ^{244}Pu, ^{244}Cm, and ^{248}Cm we have systematically overestimated the Q_4 value when compared with the single piece of experimental evidence available so far. For these nuclei as for the others, our results are, however, globally consistent with those of many different theoretical approaches. We are therefore led to the conclusion that Hartree-Fock+BCS calculations using the Skyrme *SIII* effective force do reproduce most of the available experimental data concerning the static properties of very heavy nuclei.

ACKNOWLEDGMENTS

We gratefully acknowledge many useful discussions with R. de Swiniarski and M. Brack. We would also like to thank M. Girod, G. Haouat, and Ch. Lagrange for having communicated some results prior to publication and H. Flocard for having collaborated in an early stage of this work. Finally, we are grateful to the service de calcul de la Division de Physique Théorique de l'Institut de Physique Nucléaire at Orsay for efficient and generous help in the computer calculations.

APPENDIX A: BASIS PARAMETER OPTIMIZATION, NUMERICAL ACCURACY, AND CONVERGENCE PROBLEMS

The axially symmetrical oscillator basis is entirely specified by two oscillator frequencies $\omega_\perp$ and ω_z

or equivalently by two parameters b and q:

$$q=\omega_\perp/\omega_z\ ,\quad b=\sqrt{m\omega/\hbar}\ ,$$

where

$$\omega=(\omega_\perp^2\omega_z)^{1/3}\ .$$

A careful minimization of the total energy with respect to b and q has been performed for each ground state solution. It is interesting to quantitatively determine how much the expectation values of operators other than the Hamiltonian could depend on a slight variation of b and q around their optimal values. This is exemplified in Table VI for the quadrupole and hexadecapole moments and the radii of the charge distribution of the ^{238}Pu ground state solution. For a relative variation of b of $\sim 4\%$ the total energy varies by ~ 1 MeV, whereas the charge radius is changed by less than 1%. The quadrupole and hexadecapole moments on the contrary may vary significantly (up to $\sim 1\%$ for Q_2 and to $\sim 15\%$ for Q_4). Now, for relative variations of q of $\sim 12\%$ one gets similar changes for energies and charge radii, whereas Q_2 and Q_4 are very much modified—up to $\sim 9\%$ and 22%, respectively. If a variation of the energy of 1 MeV corresponds only to a 0.1% change, it turns out, however, that through the parameter optimization process, the total energy is determined with an accuracy better than 100 keV, which leads to an upper bound for the theoretical error bars due to the basis parameters choice of a few tenth of 1% for Q_2 and of 1% for Q_4. Charge radii are then calculated within ± 0.001 fm error limits.

Neutron and proton pairing gaps in use here have been determined from systematics of odd-even binding energy differences. Not to mention systematical errors due to their extraction from a numerical finite difference treatment of available lowest quasiparticle energies, the very concept of a pairing gap constant for each single particle state carries already a signigicant amount of simplification. It is therefore adequate to evaluate the variation of the total energy and of some charge distribution moments when arbitrarily changing the pairing gap values by $\pm$ 0.2 MeV. As shown in Table VII for the ^{238}Pu ground state solution such a modification does not yield very significant changes in the energy ($|\Delta E| \lesssim 300$ keV), the charge radius ($|\Delta R_c| \lesssim 0.001$ fm), the charge quadrupole moment ($|\Delta Q_2|/Q_2 \lesssim 0.4\%$), and the charge hexadecapole moment ($|\Delta Q_4|/Q_4 \lesssim 2\%$). If one retains 200 keV as a reasonable upper bound for the error on pairing gaps, one thus sees that the corresponding uncertainties are typically of the same order of magnitude as those associated to the parameter basis optimization process.

Hartree-Fock+BCS variational equations are solved iteratively from a standard Woods-Saxon ansatz at the first iteration. The numerical convergence of the iterative process is exemplified on Fig. 10 for the total energy and the charge radius of the ^{238}Pu ground state solution. One sees that the energy is converged up to 10 keV and the radius up to 0.001 fm already at the 35th iteration. Now, the charge quadrupole Q_2 and hexadecapole Q_4 moments are converging far less rapidly as seen on Fig. 11 from the example of the ^{238}U ground state solution. It takes about 50 iterations to get Q_2 within ~ 1 fm^2 and Q_4 within 20 fm^4. All ground state properties presented in this work result from

TABLE VI. Variation ΔE of the total energy E (expressed in MeV), Δr_c of the charge radii r_c (expressed in fm), ΔQ_2 of the charge quadrupole moment Q_2 (expressed in b), and ΔQ_4 of the charge hexadecapole moment Q_4 (expressed in b^2) when changing the basis parameters around their optimal values. The notations (b,q), $(b^\pm,q)$, and $(b,q^\pm)$ refer to calculations performed with $b=0.514$ fm^{-1}, $b^\pm = b\pm 0.020$ fm^{-1}, $q=1.23$ and $q^\pm = q\pm 0.02$.

	E	r_c	Q_2	Q_4
(b,q)	−1790.3	5.947	11.13	1.216
	ΔE	Δr_c	ΔQ_2	ΔQ_4
(b^-,q)	1.2	0.000	−0.01	0.035
(b^+,q)	1.4	−0.008	0.16	0.180
(b,q^-)	1.5	−0.017	−0.99	0.267
(b,q^+)	0.4	0.001	0.35	0.020

TABLE VII. Same as Table VI for a variation of the neutron Δ_n and proton Δ_p pairing gaps around their values as determined from odd-even binding energy differences. The notations (Δ_n,Δ_p), $(\Delta_n^{\pm}\Delta_p)$, and $(\Delta_n, \Delta_p^{\pm})$ refer to calculations performed with $\Delta_n = 0.60$ MeV, $\Delta_n^{\pm} = \Delta_n \pm 0.20$ MeV, $\Delta_p = 0.74$ MeV, and $\Delta_p^{\pm} = \Delta_p \pm 0.20$ MeV.

	E	r_c	Q_2	Q_4
(Δ_n,Δ_p)	−1790.28	5.947	11.131	1.2157
	ΔE	Δr_c	ΔQ_2	ΔQ_4
(Δ_n^-,Δ_p)	0.23	−0.001	0.030	0.0116
(Δ_n^+,Δ_p)	−0.30	0.000	−0.025	−0.0145
(Δ_n,Δ_p^-)	0.21	−0.001	0.000	0.0116
(Δ_n,Δ_p^+)	−0.28	0.001	−0.020	−0.0157

at least 50 iteration calculations.

As a conclusion of the three studies presented above, it turns out that numerical errors due to the choice of optimal basis parameters and of pairing gap parameters are of a comparable magnitude. They are far smaller, however, than the discrepancies between calculated and experimental values. Moreover, the numerical errors associated with the convergence of the iterative solution of the variational equations are negligible with respect to the two above mentioned sources of uncertainty.

APPENDIX B: RADII AND QUADRUPOLE AND HEXADECAPOLE MOMENTS OF SHARP EDGED AND DIFFUSE DISTRIBUTIONS

We will first prove the following theorem: Given a distribution $\rho(\vec{r})$ and a monopole form factor $f(\vec{r})$, the convolution product of $\rho(\vec{r})$ by $f(\vec{r})$ has all its multipole moments identical to those of $\rho(\vec{r})$. The multipole moment $Q_{\lambda 0}$ of the distribution $\rho(\vec{r})$, corresponding to the operator

$$q_{\lambda 0}(\vec{r}) = r^{\lambda} Y_{\lambda 0}(\hat{r}) \tag{B1}$$

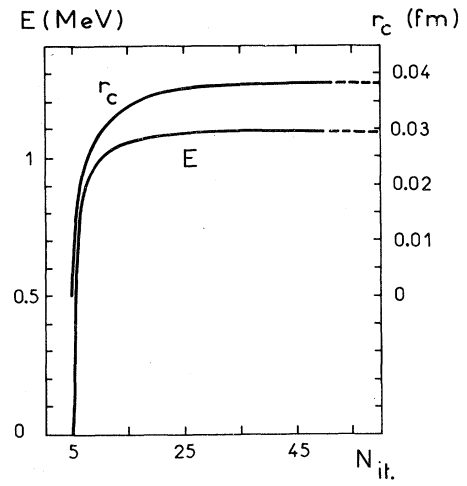

FIG. 10. Convergence of the charge radius r_c and the total Hartree-Fock+BCS energy E as a function of the number of iteration N_{it}, from a standard Woods-Saxon initial ansatz for the central mean field. These calculations have been performed for the ^{238}Pu nucleus. Radii and energies are relative to their values at $N_{it}=5$.

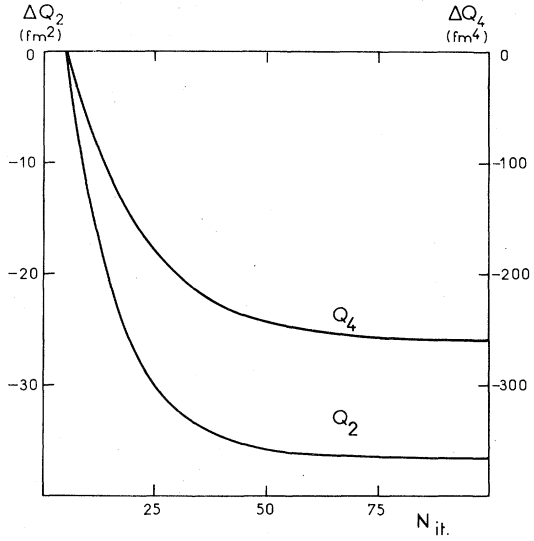

FIG. 11. Convergence of the quadrupole (Q_2) and hexadecapole (Q_4) moments for the charge distribution as functions of the number of iteration N_{it}. The calculations have been performed for the ^{238}U nucleus. We give here moments relative to their values at $N_{it}=5$.

is given by

$$Q_{\lambda 0}=\int d^3r\ \rho(\vec{r})q_{\lambda 0}(\vec{r})\ . \tag{B2}$$

Given a monopole form factor $f(\vec{r})$ normalized to unity:

$$\delta_{\lambda 0}\frac{1}{\sqrt{4\pi}}=\int d^3r\, f(\vec{r})q_{\lambda 0}(\vec{r})\ , \tag{B3}$$

one defines the multipole moment $\tilde{Q}_{\lambda 0}$ of the convoluted distribution $\rho * f$ as

$$\tilde{Q}_{\lambda 0}=\int\int d^3r\ d^3r'\ \rho(\vec{r}')f(\vec{r}-\vec{r}')q_{\lambda 0}(\vec{r})\ . \tag{B4}$$

Now $q_{\lambda 0}(\vec{r})$ may be expanded on functions $q_{\mu\nu}(\vec{r}-\vec{r}')$:

$$q_{\lambda 0}(\vec{r})=\sum_{\mu=0}^{\lambda}\sum_{\nu=-\mu}^{\mu}A_{\mu\nu}(\vec{r}')q_{\mu\nu}(\vec{r}-\vec{r}')\ , \tag{B5}$$

in such a way as to obtain, after changing one integration variable and performing the corresponding integration,

$$\tilde{Q}_{\lambda 0}=\int d^3r'\rho(\vec{r}')\frac{A_{00}(\vec{r}')}{\sqrt{4\pi}}\ . \tag{B6}$$

From Eq. (B5) one gets from letting $\vec{r}=\vec{r}'$

$$Q_{\lambda 0}(\vec{r}')=\frac{A_{00}(\vec{r}')}{\sqrt{4\pi}}\ , \tag{B7}$$

and therefore,

$$\tilde{Q}_{\lambda 0}=Q_{\lambda 0}\ , \tag{B8}$$

which proves the theorem.

One defines the rms distribution radius R of the distribution $\rho(\vec{r})$ by

$$R^2\int d^3r\ \rho(\vec{r})=\int d^3r\ |\vec{r}|^2\rho(\vec{r})\ , \tag{B9}$$

and similarly $\tilde{R}$ for the convoluted distribution by

$$\tilde{R}^2\int d^3r\ \rho(\vec{r})=\int\int d^3r\ d^3r'\ |\vec{r}|^2\rho(\vec{r}')f(\vec{r}-\vec{r}')\ , \tag{B10}$$

where the normalization integral in the left-hand side of Eq. (B10) is the same as in Eq. (B9) due to the normalization of f. Upon writing $|\vec{r}^2|$ as $|\vec{r}-\vec{r}'|^2+2\vec{r}'\cdot(\vec{r}-\vec{r}')+\vec{r}'^2$, one gets

$$\tilde{R}^2=\sigma^2+R^2\ , \tag{B11}$$

where σ^2 is defined as the rms radius of $f(\vec{r})$,

$$\sigma^2=\int d^3r\ |\vec{r}^2|f(\vec{r})\ . \tag{B12}$$

We will now briefly describe the calculations which have been performed in order to extract, from the quadrupole and hexadecapole moments (Q_2 and Q_4) of our symmetric self-consistent wave functions, standard Bohr-Mottelson β_2 and β_4 parameters. The method in use consists in finding a sharp-edged[48] liquid drop having the same quadrupole and hexadecapole moments as our self-consistent solution. The liquid drop is defined by its radius

$$R=R_0(\beta_i)g(\cos\theta,\beta_i)\ , \tag{B13}$$

where the function g is defined as usual in terms of the deformation parameters β_2, β_4 and of the angle θ between the radius and the symmetry axis by

$$g(\cos\theta,\beta_i)=1+\sum_{i=2,4}\beta_i Y_{i0}(\theta)\ . \tag{B14}$$

The volume conservation imposes that

$$R_0(\beta_i)=R_0(0)\left\{2\Big/\int_{-1}^{+1}du\,[g(u,\beta_i)]^3\right\}^{1/3}\ , \tag{B15}$$

where the spherical radius $R_0(0)$ is assumed to be proportional to $A^{1/3}$, A being the nucleon number. Consequently, the liquid drop model under consideration depends on the three parameters β_2, β_4, and r_0. The value of the latter defined by $R_0(0)=r_0A^{1/3}$, is taken from Ref. 29 ($r_0=1.2049$ fm), whereas β_2 and β_4 are determined from calculated Q_2 and Q_4 by solving the following nonlinear system of two equations:

$$Q_2=\tfrac{3}{5}\mathcal{N}\frac{[R_0(\beta_i)]^5}{[R_0(0)]^3}\int_{-1}^{+1}du\,P_2(u)[g(u,\beta_i)]^5 \tag{B16}$$

and

$$Q_4=\tfrac{3}{7}\mathcal{N}\frac{[R_0(\beta_i)]^7}{[R_0(0)]^3}\left[\frac{9}{16\pi}\right]^{1/2}\times\int_{-1}^{+1}duP_4(u)[g(u,\beta_i)]^7\ , \tag{B17}$$

where $\mathcal{N}$ is the norm of the considered density (i.e., the total number of nucleons, protons, etc, . . .) and P_2, P_4 usual Legendre polynomials. An alternative method (which has not been considered here) would have been to determine the three parameters r_0, β_2, and β_4 from self-consistent radii r and Q_2, and Q_4 moments by solving Eqs. (B16) and (B17) together with

$$r^2=\tfrac{3}{10}\frac{[R_0(\beta_i)]^5}{[R_0(0)]^3}\tfrac{3}{10}\int_{-1}^{+1}du\,[g(u,\beta_i)]^5\ . \tag{B18}$$

[1]D. Vautherin and D. M. Brink, Phys. Rev. C 5, 626 (1972).
[2]M. Beiner, H. Flocard, Nguyen Van Giai, and P. Quentin, Nucl. Phys. A238, 29 (1975).
[3]H. Flocard, P. Quentin, A. K. Kerman, and D. Vautherin, Nucl. Phys. A203, 433 (1973).
[4]M. Cailliau, J. Letessier, H. Flocard, and P. Quentin, Phys. Lett. 46B, 11 (1973).
[5]J. Sauvage-Letessier, P. Quentin, and H. Flocard Nucl. Phys. (in press)
[6]X. Campi, H. Flocard, A. K. Kerman, and S. E. Koonin, Nucl. Phys. A251, 193 (1975).
[7]X. Campi and M. Epherre, Phys. Rev. C 22, 2605 (1980).
[8]J. Libert, M. Meyer, and P. Quentin, unpublished calculations for erbium isotopes.
[9]D. Vautherin, Phys. Rev. C 7, 296 (1973).
[10]H. Flocard, P. Quentin, and D. Vautherin, Phys. Lett. 46A, 104 (1973).
[11]H. Flocard and P. Quentin, unpublished calculations for *s-d* shell nuclei.
[12]P. Quentin in *Nuclear Self-consistent Fields,* edited by G. Ripka and M. Porneuf (North-Holland, Amsterdam, 1975), p. 297.
[13]O. Bohigas, A. M. Lane, and J. Martorell, Phys. Rep. 51, 267 (1979).
[14]J. Libert, M. Meyer, and P. Quentin, Phys. Rev. 25, xxx (1982).
[15]P. Quentin and H. Flocard, Annu. Rev. Nucl. Part. Sci. 28, 523 (1978).
[16]M. Beiner (private communication).
[17]D. W. L. Sprung, S. G. Lie, M. Vallières, and P. Quentin, Nucl. Phys. A236, 37 (1979).
[18]A. H. Wapstra and K. Bos, At. Data Nucl. Data Tables A19, 177 (1977).
[19]H. Flocard, P. Quentin, D. Vautherin, M. Véneroni, and A. K. Kerman, Nucl. Phys. A231, 176 (1974).
[20]M. Brack and P. Quentin, in *Nuclear Self-Consistent Fields,* edited by G. Ripka and M. Porneuf (North-Holland, Amsterdam, 1975), p. 353.
[21]H. C. Pauli, Phys. Rep. 7, 35 (1973).
[22]P. Möller, S. G. Nilsson, and J. R. Nix, Nucl. Phys. A229, 292 (1974); P. Möller and J. R. Nix, *ibid.* A292, 269 (1974).
[23]S. G. Nilsson, C. F. Tsang, A. Sobiczewski, Z. Szymański, S. Wycech, C. Gustafson, I.-L. Lamm, P. Möller, and B. Nilsson, Nucl Phys. A131, 1 (1969).
[24]C. Gustafson, I.-L. Lamm, B. Nilsson, and S. G. Nilsson, Ark. Fys. 36, 613 (1967).
[25]J. Libert, M. Meyer, and P. Quentin, Phys. Lett. 95B 175 (1980).
[26]The three phenomenological well parmetrizations used in Fig. 7 are due to H. C. Pauli (Ref. 21), to P. Möller, S. G. Nilsson, and J. R. Nix (Ref. 22), and to U. Mosel and H. W. Schmitt [Nucl. Phys. A165, 13 (1971)].
[27]P. Quentin, Ph.D. thesis, Université d'Orsay, 1975 (unpublished).
[28]See also in the simplified case where the convoluted density is obtained by folding a step function with a monopole form factor, K. T. R. Davies and J. R. Nix, Phys. Rev. C 14, 1977 (1976).
[29]W. D. Myers and W. J. Swiatecki, Nucl. Phys. 81, 1 (1966).
[30]Å Bohr and B. Mottelson, *Nuclear Structure* (Benjamin, New York, 1969), Vol. 1.
[31]W. Bertozzi, J. Friar, J. Heisenberg, and J. W. Negele, Phys. Lett. 41B, 408 (1972).
[32]From muonic atom x-ray measurements, D. A. Close *et al.* [Phys. Rev. C 17, 1433 (1978)] have fitted deformed Fermi-type charge density parameters for the ^{232}Th and ^{238}U nuclei [see Eq. (8) and Table VIII in this ref.] from which we have computed the "experimental" charge radii.
[33]P. H. Stelson and L. Grodzins, Nucl. Data Tables A1, 21 (1965).
[34]F. K. McGowan, C. E. Bemis, Jr., J. L. C. Ford Jr., W. T. Milner, R. L. Robinson, and P. H. Stelson, Phys. Rev. Lett. 27, 1741 (1971); C. E. Bemis Jr., F. K. McGowan, J. L. C. Ford Jr., W. T. Milner, P. H. Stelson, and R. L. Robinson, Phys. Rev. C 8, 1466 (1973); C. E. Bemis Jr., W. T. Milner, and F. K. McGowan, *ibid.* 16, 1686 (1977). The figures quoted in Table III have been taken from the model dependent analysis of data performed in Phys. Rev. C 16, 1686 (1977).
[35]D. L. Hendrie, B. G. Harvey, J. R. Meriwether, J. Mahoney, J. C. Faivre, and D. G. Kovar, Phys. Rev. Lett. 30, 571 (1973).
[36]P. David, J. Debrus, H. Essen, F. Lübke, H. Mommsen, R. Schoenmackers, W. Soyez, H. V. v. Geramb, and E. F. Hefter, Z. Phys. A 278, 281 (1976).
[37]J. M. Moss, Y. D. Terrien, R. M. Lombard, C. Brassard, J. M. Loiseaux, and F. Resmini, Phys. Rev. Lett. 26, 1488 (1971).
[38]I. Brissaud, G. Berrier-Ronsin, J. Cameron, R. Frascaria, J. Kalifa, G. Bagieu, and R. de Swiniarski, Z. Phys. A 293, 1 (1979).
[39]T. Cooper, W. Bertozzi, J. Heisenberg, S. Kowalski, W. Turchinetz, C. Williamson, L. Cardman, S. Fivozinski, J. Lightbody Jr., and S. Penner, Phys. Rev. C 13, 1083 (1976).
[40]J. P. Davidson, D. A. Close, and J. J. Malanify, Phys. Rev. Lett. 32, 337 (1974).
[41]D. A. Close, J. J. Malanify, and J. P. Davidson Phys. Rev. C 17, 1433 (1978).
[42]G. Haouat, J. Lachkar, Ch. Lagrange, Y. Patin, J. Sigaud, and R. E. Shamu, Bruyères le Chatel, Report NEANDC(E) 196"L", 1978; G. Haouat and Ch.

Lagrange (private communication).

[43]P. Quentin, I. Brissaud, and R. de Swiniarski, Z. Phys. A298, 37 (1980).

[44]J. W. Negele and G. Rinker, Phys. Rev. C 15, 1499 (1977).

[45]M. Girod and D. Gogny (private communication).

[46]F. A. Gareev, S. P. Ivanova, and V. V. Pashkevich, Yad Fiz. 11, 1200 (1970) [Sov. J. Nucl. Phys. 11, 667 (1970)].

[47]M. Brack, T. Ledergerber, H. C. Pauli, and A. S. Jensen, Nucl. Phys. A234, 185 (1974).

[48]The sharp edged character of the drop is not a limitation in so far as one may consider that the diffuseness of the density distribution could be obtained by convoluting a step function with a monopolar form factor, and thence use the theorem proven above [see Eq. (B8)].